Investigation of Ordered ds-DNA Monolayers on Gold Electrodes

Rong-Ying Zhang,[†] Dai-Wen Pang,*[,†] Zhi-Ling Zhang,[†] Jia-Wei Yan,[‡] Jian-Lin Yao,[‡] Zhong-Qun Tian,[‡] Bing-Wei Mao,[‡] and Shi-Gang Sun[‡]

Department of Chemistry, Wuhan University, Wuhan 430072, P. R. China, and State Key Laboratory for Physical Chemistry of Solid Surfaces, Department of Chemistry, Xiamen University, Xiamen 361005, P. R. China

Received: March 23, 2002; In Final Form: August 30, 2002

Double-stranded DNA(poly(dA)$_{30}$·poly(dT)$_{30}$) -modified gold electrodes, prepared by air-drying/adsorption method, have been investigated by various techniques, including cyclic voltammetry (CV), quartz crystal microbalance (QCM), electrochemical scanning tunneling microscopy (EC−STM), and surface-enhanced Raman scattering spectroscopy (SERS). CV and QCM results show that an average surface coverage of (7.5 ± 0.2) × 10^{-12} mol cm^{-2} was obtained for poly(dA)$_{30}$·poly(dT)$_{30}$-modified gold electrodes, close to the value for a saturated monolayer of ds-DNA lying flat on surfaces. EC−STM was used to evidence directly that ds-DNA forms a highly ordered and compact monolayer film on the gold substrate, whereas single-stranded DNA(poly(dT)$_{30}$) adopts a coiled configuration and, therefore, cannot form an ordered structure on the gold substrate. Moreover, it was demonstrated, for the first time, by SERS experiments that partial denaturation of duplexes occurs arising from the different interfacial orientations of A and T bases on the gold electrode surface. The adsorptive nature of the surface-bound ds-DNA was also elucidated, which results in the obtained DNA-modified gold surfaces stable in a wide range of potentials.

Introduction

Heterogeneous DNA sensors (i.e., solid surface-immobilized DNA sensors) have many potential applications in modern molecular biology, e.g., DNA sequencing, gene mapping, molecular diagnostics, and analysis of DNA−ligand interactions. Developers employed various methods, such as adsorption, copolymerization, complexation, covalent attachment, etc., for immobilization of DNA on different substrates.[1−5] Some of these methodologies are suitable for chemically modified oligonucleotides. For example, thiol-tethered oligonucleotides can form a highly oriented self-assembled monolayer on gold substrates via Au−S bond.[6,7] Meanwhile, for those relatively large and/or unmodified DNA molecules, they can also be immobilized on solid substrates based on different surface chemical reactions. Millan et al.[8] coupled ss-DNA to carbon paste electrodes via carbodiimide-mediated formation of a phosphoramidate bond between 5'-terminal phosphate of the DNA and the terminal amino group of octadecylamine anchored on carbon paste. Besides, many methods include the use of functionalized alkanethiol to form SAM on substrates as base layer, and subsequently DNA is immobilized via covalent coupling of the amino group of base[9] or phosphate of deoxyribose-phosphate backbone[10] to the functionalized SAMs.

Although development of methods for controlled immobilization of oligonucleotides on surfaces is still key to DNA biosensor design, much attention has been paid to understanding the relation between the microenvironment on a DNA-modified electrode and the merit of it. The optimization of many important parameters,[4,6,11] such as interface/solution condition, time for DNA immobilization, surface coverage, orientation of immobilized DNA, etc., will benefit the analysis of hybridization reaction or ligand binding. Numerous sensitive surface analytical techniques,[4,6,7,9,12,13] such as surface plasmon resonance (SPR), scanning probe microscopy (SPM), X-ray photoelectron spectroscopy (XPS), QCM, attenuated total reflectance Fourier transformation infrared spectroscopy (ATR-FTIR), and neutron reflectivity, were therefore introduced to signal detection and analysis.

We previously explored a simple method for preparing DNA-modified electrode−air-drying/adsorption method, and on the basis of that, a micromethod for the study of interactions between surface-bound DNA and redox-active molecules in solution[14,15] was also developed. Compared with those earlier solution methods proposed by Bard et al.,[16] this method is characterized by its simplicity, reliability, and microscale sample requirements. It is of obvious importance to clarify the mechanism of DNA immobilization. In this paper, gold electrodes were modified with relatively short and uniform ds-DNA (poly(dA)$_{30}$·poly(dT)$_{30}$) by air-drying/adsorption method and then were characterized by CV, QCM, EC−STM, and SERS techniques. Compared with calf thymus DNA, relatively short and uniform poly(dA)$_{30}$·poly(dT)$_{30}$ not only makes possible and simplifies the quantification of surface coverage but also is helpful in applying EC−STM and SERS techniques to investigate the orientation and adsorption of DNA molecules on gold substrates, which is known to be very important for DNA biosensor design.

Experimental Section

Materials. A quantity of 30-mer single-stranded polydeoxyadenosine and polydeoxythymidine, obtained from GIBCOBRL, were used as received. The poly(dA)$_{30}$·poly(dT)$_{30}$ duplex (molecular weight, 19 384) was prepared by mixing poly(dA)$_{30}$

* To whom correspondence should be addressed. E-mail: dwpang@whu.edu.cn.
[†] Wuhan University.
[‡] Xiamen University.

10.1021/jp025817o CCC: $22.00
Published on Web 10/05/2002

and poly(dT)$_{30}$ stock solution at a molar nucleotide ratio of 1:1 in 1 M NaCl solution buffered with TE (10 mM pH 7.4 Tris-HCl + 1 mM EDTA) in a 52 °C water bath for 90 min, followed by allowing it to cool slowly at room temperature (1∼2 h). Tris-(1,10-phenanthroline) cobalt(II) was used as received. Other chemicals used were of analytical reagent grade without further purification. The water used was deionized and then passed through a Milli-Q water purification system (Millipore Corp., Bedford, MA).

Preparation of DNA-Modified Gold Electrodes. Gold electrodes used for CV and SERS experiments were purchased from CH Instruments, Co. Before use, they were polished with alumina polishing powder (Buehler) from 1 μm down to 0.05 μm, followed by sonicate in water and cyclic scanning in 0.5M H_2SO_4 between −0.2 V and +1.5 V(vs SCE) till obtaining stable redox peaks of Au. QCM crystals used for the quantification of immobilized DNA were 9 MHz, AT-cut shear mode quartz crystal with Au deposited on both sides. The bare QCM crystal electrode was cleaned with a solution of 25% H_2O_2/75% H_2SO_4 (piranha solution) to remove organic adsorbate impurities. *CAUTION: Piranha solution reacts violently with organic solvents and is a skin irritant. Extreme caution should be exercised when handling piranha solution.* A flame-annealed gold (111) substrate used for EC−STM was made as previously reported.[17] Before modification with desired DNA, it was first electrochemically polished[18] to remove organic adsorbate impurities, rinsed with water three times, and subsequently dried in an N_2 stream. For SERS experiments, the mechanically polished gold electrodes were ex-situ electrochemically pretreated according to Weaver et al.[19] before immobilization of ds-DNA, so as to obtain large-scale rough particles of the order of 100 nm diameter, which was proven to be helpful to yielding unusually strong SERS. The typical procedure for preparing DNA-modified gold electrodes is as follows.[14,15,17] A droplet of 2∼5 μL (0.2 μg/μL) ds-DNA or ss-DNA solution was deposited onto the cleaned electrode surface and then dried in air. Then the electrode was soaked in water for at least 4 h and rinsed with water to remove any unadsorbed DNA; thus, a ds-DNA or ss-DNA modified gold electrode was obtained. The resulting electrode was denoted as ds-DNA/Au or ss-DNA/Au.

Procedures. *(a) Cyclic Voltammetry.* Voltammetric measurements were performed with a CHI 660A electrochemical workstation (Shanghai Chenhua Co.). A three-compartment cell was used for the experiments. A bare gold or ds-DNA modified gold electrode with a microscopic area of about 0.063 cm^2 served as the working electrode, a platinum wire served as the counter electrode, and a saturated calomel electrode (SCE) served as the reference electrode. All solutions were deaerated with highly pure nitrogen, and the experiments were carried out at 25°C.

(b) QCM. QCM measurements were conducted on a QCA917 type quartz crystal microbalance (SEIKO EG&G Co.) using dried crystals, because the resonance frequency decreases linearly with the increasing mass of adsorbate on a QCM electrode at nanogram level in the gas phase. The quartz crystal electrode was sealed in an electrolytic cell with a rubber casing, and one exposed side with a geometric area of 0.2 cm^2 was used for frequency measurements and DNA immobilization. The roughness factor was 1.5 ($R = Q_0'/Q_0$, Q_0' was the electric charge for the oxidation of Au surface obtained by integrating the $j-E$ curve in the oxide reduction region and Q_o was a reference electric charge as 420 μC cm^{-2}). When the frequency change, df, is less than 2% of the fundamental frequency, Sauerbrey equation for gas phase is described as

$$df = -C_f dm$$

where $df = f - f_0$, dm (g cm^{-2}) is the mass change, and C_f is the mass sensitivity factor. For a 9 MHz, AT-cut shear mode QCM, $C_f = 0.178 \times 10^9$ Hz g^{-1} cm^2, the noise level was less than ±4 Hz at 25 °C, and the standard deviation of the frequency was 10 Hz for 8 h under the same conditions. Before experiments, a piranha-solution-cleaned crystal was sonicated in acetone and water for 3 min and dried over a stream of N_2 gas. The saturated resonance frequency of the bare crystal was first determined and subsequently monitored after the crystal was modified with ds-DNA (as described above).

(c) EC−STM. EC−STM measurements were carried out on a Nanoscope IIIa (Digital Instruments, Co) in the constant current mode. An electrochemically etched tungsten tip was used in the measurement, the bias voltage was in the range of −0.4 to −0.55 V, and the tunneling current was 0.25∼1.5 nA. Images of ds-DNA/Au and ss-DNA/Au were obtained in 10 mM Tris-HCl/10mM NaCl buffer (pH 7.4) over a potential range of −0.9 to +0.6 V (vs SCE), and the potential was changed from 0 V toward negative and positive direction by 0.1 V each time.

(d) Raman and SERS. Conventional Raman and surface-enhanced Raman scattering (SERS) spectra of poly(dA)$_{30}$·poly-(dT)$_{30}$ were acquired on a LabRamI Confocal MicroRaman System (Dilor, France) with Notch Filter and a low noise CCD detector, which is characterized by allowing the use of a single short focal length monochromator (0.25 nm) and relatively high sensitivity. The confocal microscope was equipped with a long focal (50×) camera lens. The excitation source was the 632.8 nm line from a He−Ne laser (∼10 mW power at the sample). A total scan of 100 s × 3 times was accumulated to achieve an acceptable signal-to-noise ratio for the conventional Raman spectra. The measurements of the potential dependence of the SERS spectra were performed in a medium of 10 mM KNO_3, with Pt wire and saturated calomel electrode (SCE) as counter electrode and reference electrode, respectively. The potential of the working electrode was controlled using a PARC 173 potentiostat. A total scan of 40 s × 3 times was accumulated to achieve an acceptable signal-to-noise ratio and reduce the influence of photochemical reactions on gold electrode to the minimum limit.

Results and Discussion

CV Characterization of ds-DNA/Au Electrodes. Potassium ferricyanide ($K_4Fe(CN)_6$), hexaammineruthenium(III) (RuHex), and tris(1,10-phenanthroline) cobalt(II) ($[Co(Phen)_3]^{3+/2+}$) are known to be the common electroactive species for qualitatively or quantitatively probing DNA immobilized on electrode surfaces. In this work, $[Co(Phen)_3]^{3+/2+}$ was employed to probe whether the DNA molecules had been anchored on the electrode surface or not. As shown in Figure 1, there was no obvious CV response for 20 μM $[Co(Phen)_3]^{3+/2+}$ at the bare gold electrode due to the low concentration, whereas a pair of obviously large redox peaks at $E^{o\prime}$ of about 0.119 V, with $\Delta E_p = 43$ mV were generated on the ds-DNA/Au electrode, which is due to the accumulation of $[Co(Phen)_3]^{3+/2+}$ into the DNA layer arising from the strong interaction between $[Co(Phen)_3]^{3+/2+}$ and the surface-bound DNA. Moreover, the peak current was directly proportional to the scan rate, v, which is characteristic of a surface process. The above results suggest that ds-DNA can be immobilized on the gold electrode via air-drying/adsorption method.

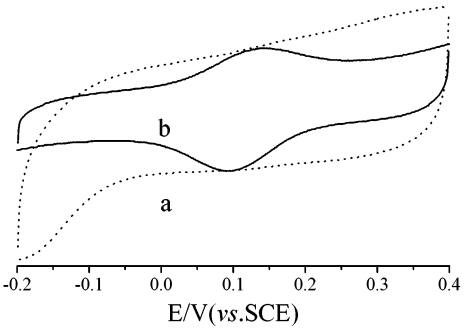

Figure 1. Cyclic voltammograms of 20 μM $[Co(Phen)_3]^{3+/2+}$ in 5 mM pH 7.1 Tris-HCl buffer containing 5 mM NaCl (a) at a bare gold electrode and (b) at a ds-DNA/Au electrode. Scan rate: 0.05 V/s.

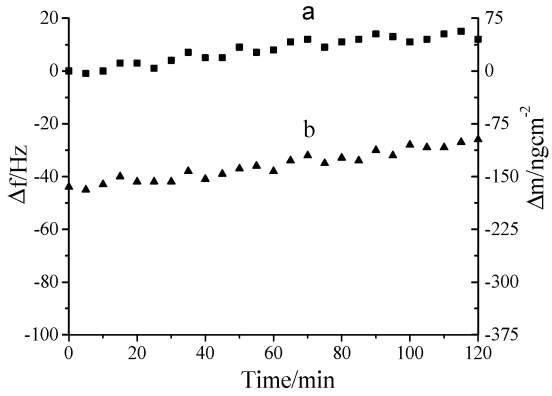

Figure 2. Typical time dependencies of the saturated resonance frequency of (a) a bare gold crystal electrode and (b) a poly(dA)$_{30}$·poly(dT)$_{30}$-modified gold crystal electrode in air phase.

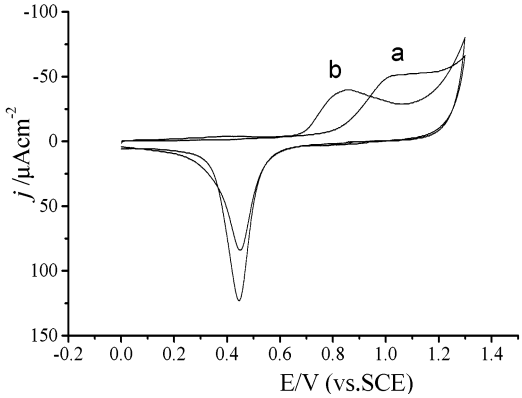

Figure 3. Cyclic voltammograms of a ds-DNA/Au electrode in 0.1 M PBS, pH 7.0 (a) the first scan and (b) the second scan. Scan rate: 0.03V/s.

Quantification of ds-DNA Immobilized on Gold Electrodes. The surface coverage of DNA on the electrode can be calculated from the difference of resonance frequency between the bare gold and DNA-modified gold electrode in gas phase. Figure 2 shows time-dependencies of the saturated resonance frequency of both bare gold (curve a) and ds-DNA modified gold electrode (curve b) at a sampling time interval of 5 min under the same conditions. A surface coverage of 150 $\pm$ 15 ng cm^{-2}, corresponding to (7.7 $\pm$ 0.8) $\times$ 10^{-12} mol cm^{-2} 30-mer ds-DNA, was calculated from the Δf value of -40 ± 4 Hz.

The surface coverage of immobilized ds-DNA can also be attained from the electro-oxidation charge of dA or dG residue[20] on a ds-DNA/Au electrode. Figure 3 represents the voltammogram of a poly(dA)$_{30}$·poly(dT)$_{30}$-modified gold electrode in 0.1 M pH 7.0 PBS buffer solution, where curve a and b are the first and second scan, respectively. It can be seen that the beginning of oxidation of gold substrate is only retarded but not prevented by the adsorption of ds-DNA and that the oxidation reaction of ds-DNA appears at more positive potentials. An oxidation charge (Q) of 127 μC cm^{-2} can be calculated for the surface-bound poly(dA)$_{30}$·poly(dT)$_{30}$ from the difference of electrooxidation charge between curve a and b, a surface coverage of (7.4 $\pm$ 0.4) $\times$ 10^{-12} mol cm^{-2} 30-mer ds-DNA can therefore be determined by assuming the transfer of 6 electrons per AT base pair.[20]

TABLE 1: Surface Coverage, Obtained by Different Methods, of Poly(dA)$_{30}$·Poly(dT)$_{30}$ on Gold

method	coverage (mol cm^{-2})
theoretical calculation	8.1×10^{-12}
QCM	$(7.7 \pm 0.8) \times 10^{-12}$
CV	$(7.4 \pm 0.4) \times 10^{-12}$

On the other hand, provided that ds-DNA is adsorbed flat on the gold substrate in a saturated monolayer, a surface coverage can be calculated to be about 8.1 $\times$ 10^{-12} mol cm^{-2} from the footprint area (width $\times$ length) of 2040 Å^2 for the 30-mer duplex. Table 1 gives the surface coverage results of ds-DNA calculated by different methods. Obviously, the value of coverage obtained by QCM is close to that by CV, and both the values are a little less than that obtained from the theoretical estimation. EC−STM results, presented below, will be helpful to understanding the rationality. Electrostatic repulsion between the negatively charged deoxyribose−phosphate backbones of neighboring duplexes will result in some balance spacing instead of thoroughly compact arranging, which causes the surface coverage of ds-DNA obtained from the experiments a little less than the value obtained from the theoretical calculation.

EC−STM Images of ds-DNA-Modified Au (111). Parts a and b of Figure 4 show the top-view EC−STM images of bare gold(111) and poly(dA)$_{30}$·poly(dT)$_{30}$/Au(111), respectively, from which some direct evidence on the ds-DNA/Au surface structure can be obtained. First, ds-DNA molecules lie flat on the surface and give rodlike images, where the contour of DNA chains appear to be linear instead of freely coiled and the long axis of ds-DNA chains run parallel to the surface. This means that the ds-DNA was anchored at many surface sites along its entire length instead of with only a single end "dangling" from the surface.[21] Moreover, neighboring linear ds-DNA molecules appear not to be randomly oriented but parallel to one another on the surface. The diameter of the duplexes were measured to be 2 $\pm$ 0.3 nm, which is close to the value of 2 nm for a B-type DNA reported by Watson and Crick.[22] Second, a compact and saturated monolayer rather than a multilayer or submonolayer structure was observed. The reason for this observation may be elucidated below. Electrostatic repulsion between neighboring negatively charged deoxyribose−phosphate backbones would cause excess ds-DNA molecules that adsorbed on the top-layer through weak and physical sorption to depart away and go into water when the ds-DNA modified electrodes are pretreated with water, forming a saturated monolayer rather than a multilayer.[17] Third, the ordered structure of ds-DNA on gold surfaces is stable over a wide range of potentials because images similar to Figure 4b can always be obtained over a potential range of +0.6 to −0.9 V (vs SCE, not shown). The single-crystal structure of gold tends to be destroyed at potentials higher than +0.6 V, and disturbance of hydrogen evolution will occur at potentials lower than −0.9 V in the present case. Therefore, the experiments at potentials higher than +0.6 V and lower than −0.9 V were not made. As a comparison, ss-DNA (poly(dT)$_{30}$)/Au(111) prepared by the same method gave very different images, which is shown by Figure 4c. It seems that ss-DNA prefer to adsorbing

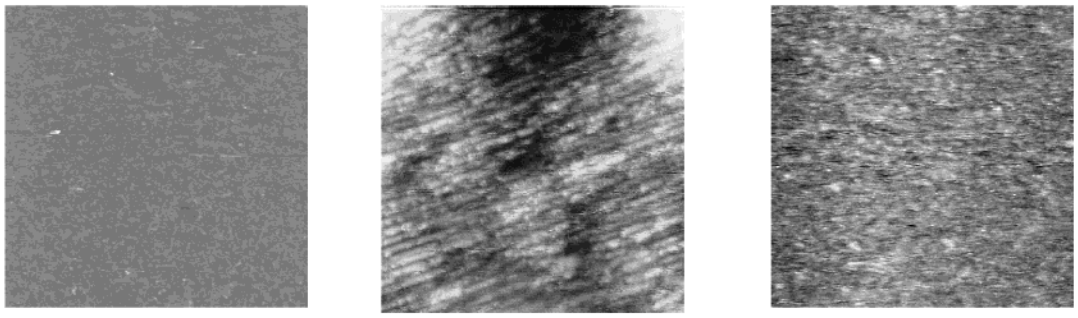

Figure 4. (a) Top-view EC−STM image of Au(111) obtained in 10 mM pH 7.4 Tris-HCl buffer containing 10 mM NaCl(constant-current mode). Scan area, 100 × 100 nm^2; *z* range, 0.15 nm; $E_{tip} = -530$ mV, $I_t = 1.1$ nA, $E = -0.2$ V (vs SCE). (b) Top-view EC−STM image of poly(dA)$_{30}$·poly(dT)$_{30}$ modified Au(111) obtained in 10 mM pH 7.4 Tris-HCl buffer containing 10 mM NaCl (constant-current mode). Scan area, 50 × 50 nm^2; *z* range, 0.84 nm; $E_{tip} = -550$ mV, $I_t = 0.25$ nA, $E = -0.7$ V (vs SCE). (c) Top-view EC−STM image of poly(dT)$_{30}$ modified Au(111) obtained in 10 mM pH 7.4 Tris-HCl buffer containing 10 mM NaCl(constant-current mode). Scan area, 50 × 50 nm^2; *z* range, 0.30 nm; $E_{tip} = -480$ mV, $I_t = 0.67$ nA, $E = -0.1$ V (vs SCE).

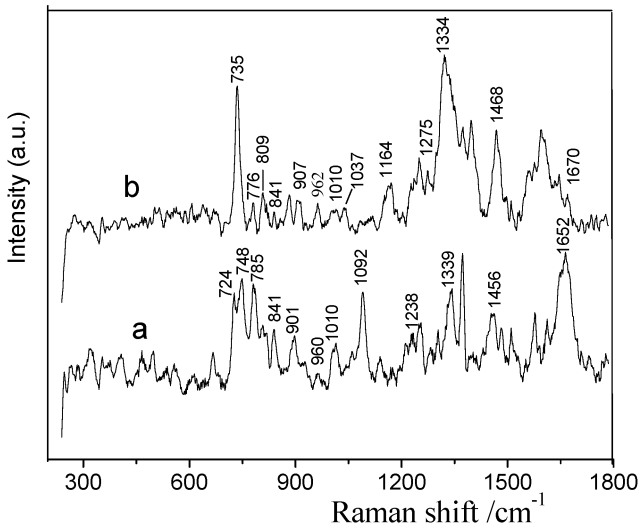

Figure 5. (a) Conventional Raman spectrum of 4mM poly(dA)$_{30}$·poly(dT)$_{30}$ in TE containing 1 M NaCl; (b) SERS spectrum of poly(dA)$_{30}$·poly(dT)$_{30}$/Au.

on the gold surface in a freely coiled form and give densely packed blob-like images due to lack of Watson−Crick hydrogen bonding (which could maintain a relatively rigid structure for ds-DNA).

The arrangement of ds-DNA on gold surfaces may therefor be regarded as "self-assembly of ds-DNA", which is different from the usually conceptual "self-assembly".[21] Braun and co-workers[23] constructed functional circuits at nanoscale level using DNA as a template for the vectorial growth of conductive silver wire. The ordered and stable DNA monolayer prepared in this paper not only can be used for studying interactions between DNA and other species[14,15] but also could be used as nanoscale template for further assembly of ordered and functionalized nanomaterials. On the basis of the specific binding of some species to the surface-bound ds-DNA and selective attachment of other species to the bare gold substrate, ordered structures of functionalized nanomaterials could be obtained at nanoscale level with ds-DNA templates of varying length depending on different demands.

Characterization of ds-DNA on Gold Surfaces by Raman and SERS. Curve a in Figure 5 shows the conventional Raman spectra of 4 mM poly(dA)$_{30}$·poly(dT)$_{30}$ solution. The bands at 841 and 1092 cm^{-1} are assigned to asymmetric −O−P−O− and symmetric PO_2^- stretching vibrations, respectively. The

TABLE 2: Assignments of the Characteristic Raman Bands of Poly(dA)$_{30}$·Poly(dT)$_{30}$[a]

band /cm^{-1}		
Raman	SERS	assignment
724	735	A (totally symmetric stretching)
748	776	T (totally symmetric stretching)
785		υ_s(−O−P−O-)
841	841	υ_{as}(−O−P−O-)
901	907	deoxyribose
960	962	−NH_2 group on A ring
1010	1010	deoxyribose
	1037	−NH_2 group on A ring
1092		$\upsilon_s(PO_2^-)$
	1164	-NH_2 group on A ring
1238	1275	T (skeletal vibration) + β(CH)
1339	1334	A (skeletal vibration)
1456	1468	deoxyribose
1652	1670	υ(C═O)$_T$

[a] υ, stretching; *s*, symmetric; *as*, asymmetric; β, bending; A, adenine; T, thymine.

furanose ring was therefore identified as being in the S-pucker, which is characteristic of a B-type DNA.[24] Besides, two relatively strong bands at 724 and 748 cm^{-1} are attributed to the totally symmetric stretching vibration[25] of adenine (A) and thymine (T) residues, respectively. The corresponding skeletal vibrations at 1339[26] and 1238 cm^{-1} [25] were observed, and a strong band at 1652 cm^{-1} [27] is attributed to the T C_4═O double bond stretching vibration mode (listed in Table 2).

Curve b in Figure 5 is the SERS spectrum of poly(dA)$_{30}$·poly(dT)$_{30}$ on an ex situ roughened gold electrode at open circuit prepared by the air-drying/adsorption method. It can be seen that distinct changes in the number, shift, intensity, and width of bands occurred for the ds-DNA molecules adsorbed on gold electrodes because of the change in the molecular polarizability. The totally symmetric stretching mode of the A ring gets enhanced and shifts upward to 735 cm^{-1} in the SERS spectrum, whereas that of the T ring, sensitive to changes in the chemical surroundings and usually shifting upward to 776 cm^{-1} [25] in SERS, is very weak in curve b. Similar results have also been observed by Fang et al.[27] for poly[dA]·poly[dT] adsorbed at an ex situ roughened silver electrode, which was explained as the result of more distant from the metal surface of T rings caused by the more favorable adsorption of the large A rings. We consider that, for the helical DNA duplexes that adsorbed flat on the electrode surface, the chance for the base A and T to be close to or to be far from the electrode surface is equal.

Therefore, the different enhancement of the same vibration mode for adenine and thymine residues, in the present case, should be the results of different orientation for them on the electrode surface.

It is known that, usually much more intense scattering can be observed when the laser polarization is aligned along the long axis of an ellipsoidal particle, which is the most polarizable direction. Therefore, the above results indicate, to some extent, that the A ring plane of ds-DNA may be perpendicular to the surface, but the T ring plane might be oriented parallel or approximately parallel to the surface. This assumption is supported by another evidence. The skeletal vibration of the A ring at 1339 cm^{-1} is remarkably enhanced in SERS, whereas the T ring stretching vibration combined with CH bending at 1238 cm^{-1}, which usually shifts upward to near 1275 cm^{-1} [25] in SERS, is not surface-enhanced markedly in the SERS spectrum. By comparing the adsorption behavior of four types of bases on Ag electrodes, Otto and co-workers[25] concluded that the intensity and width of C═O vibration band are sensitive to its orientation with respect to the surface. Therefore, the C═O vibration mode will be enhanced in the case that the T ring plane is oriented perpendicular to the electrode surface via the interaction between C═O and the surface. However, herein the C═O vibration was not surface-enhanced markedly in SERS, further suggesting that T rings are not perpendicular to the electrode surface, but interact with the surface through $\pi-$electron bonding or in other fashion. The three new bands respectively at 962, 1037, and 1164 cm^{-1}, according to Otto et al.,[25] are attributed to the vibration of the external amino groups on A rings, suggesting intensively that the A ring plane is perpendicular to the gold surface via the coordination of the $-NH_2$ group to the gold substrate. It is more reasonable for this coordination to arise from the nonbonded electron pair of $-NH_2$ instead of the hydrogen atoms, as proposed by Brabec et al.[28] The bands centered near 785[29] and 1092 cm^{-1} in conventional Raman, assigned to the totally symmetric stretching mode of diester phosphate and anionic PO_2^-, respectively, almost vanished completely in SERS, which is attributed to changes in the vibration symmetry of phosphate group, suggesting that there exists some strong interaction between phosphate groups and the electrode surface. Comparing curve a with curve b, it is worthy to note that there are no obvious differences for the bands at 901, 1010, and 1456 cm^{-1} assigned to deoxyriboses,[29,30] suggesting that deoxyriboses do not interact directly with the electrode surface and therefore play a minor role for the adsorption of ds-DNA on gold surfaces.

The above results have demonstrated that, using the air-drying/adsorption method, ds-DNA molecules are immobilized on gold surfaces via the chemisorption of bases and phosphate groups at gold substrates. Moreover, partial denaturation occurs for the surface-bound ds-DNA, which is demonstrated below. The 841 cm^{-1} band, characteristic of B-type DNA, is weak in the SERS spectrum compared to that in the conventional Raman spectra, whereas a moderate strong band, characteristic of $C_{3'-endo}$ (N-type) form nucleic acids,[24] appears at 809 cm^{-1}, which means that the different orientations for adenine and thymine residues on the electrode surface influence on the pucker of the deoxyribose coupled to the phosphate group and result in a partial denaturation of the surface-bound ds-DNA molecules.

Further, the SERS behavior of individual poly$(dA)_{30}$ and poly$(dT)_{30}$ was investigated. Curve a in Figure 6 depicts the SERS spectrum of poly$(dA)_{30}$ on the ex situ roughened gold electrode at open circuit. It can be seen that the ring breathing vibration

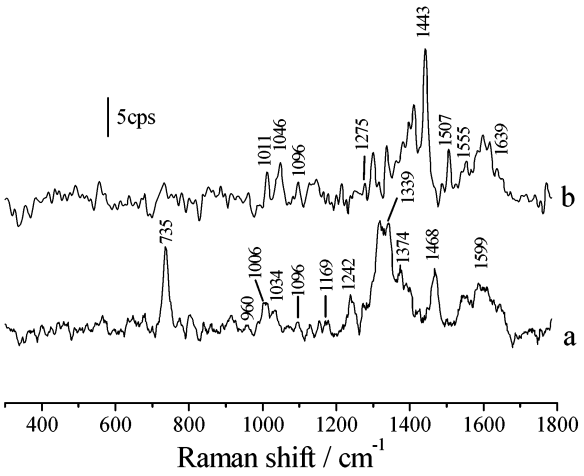

Figure 6. (a) SERS spectra of poly$(dA)_{30}$ on a roughened gold electrode at open circuit; (b) SERS spectra of poly$(dT)_{30}$ on a roughened gold electrode at open circuit.

at 735 cm^{-1} and the skeletal vibration at 1339 cm^{-1} of A rings were still remarkably enhanced, and the vibrations ascribed to the $-NH_2$ groups at 960, 1034, and 1169 cm^{-1} were surface-enhanced as well. This means that, similar to the duplex poly$(dA)_{30}$·poly$(dT)_{30}$, A ring planes on single-stranded poly$(dA)_{30}$ still prefer to be perpendicular to the gold surface. Curve b is the SERS spectrum of poly$(dT)_{30}$ on the ex situ roughened gold electrodes at open circuit; none of the ring breathing vibration at 776 cm^{-1} and the skeletal stretching vibration at 1275 cm^{-1} of T ring, together with the obviously enhanced stretching vibration of C═O group at 1670 cm^{-1}, is also analogous to the results for duplex poly$(dA)_{30}$·poly$(dT)_{30}$. Besides, the bending vibrations of C5$-CH_3$ at 1443 cm^{-1} [25] and $-$NH at 1507 cm^{-1} [25] in the region of single-bond stretching vibrations were surface enhanced remarkably. These results confirm that T ring planes were still lying flat on the gold substrate. Additionally, the enhancement effect for the vibrations related to the deoxyribose$-$phosphate backbones was also the same as that for the duplex poly$(dA)_{30}$·poly$(dT)_{30}$. Therefore, it can be concluded that, although ss-DNA was adsorbed on the gold substrate in an unordered and coiled configuration because of the absence of hydrogen bonding as formed between the complementary strands of duplex DNA (as discussed in the above STM section), the adsorption molecular mechanisms for both ds- and ss-DNA are the same, and the interfacial orientations of bases on the substrate are mainly determined by the nature of the bases themselves.

Figure 7 parts A and B shows the potential dependencies of poly$(dA)_{30}$·poly$(dT)_{30}$ adsorbed at the ex situ roughened gold electrode from the open circuit potential toward the negative and positive direction, respectively, which is remarkably different from that of the DNA adsorbed at the ex situ roughened silver electrode via polarization at different potentials in DNA solution.[24,27] First, as shown in Figure 7A, the adsorption of poly$(dA)_{30}$·poly$(dT)_{30}$ on the electrode surface was not influenced by the electrostatic repulsion between the negatively charged phosphate$-$deoxyribose backbone and the negatively charged electrode and would not desorb away from the electrode surface, even when the electrode potential is far more negative than the zero charge potential of gold electrode($\varphi_{pzc} \sim 0.2$ V).[31] Meanwhile, it can be seen from Figure 7B that the enhancement of almost all of the vibration modes tends to weaken along with the accumulation of positive charge on the electrode surface. These results suggest intensively that the immobilization of ds-DNA on a gold electrode using air-drying/adsorption method

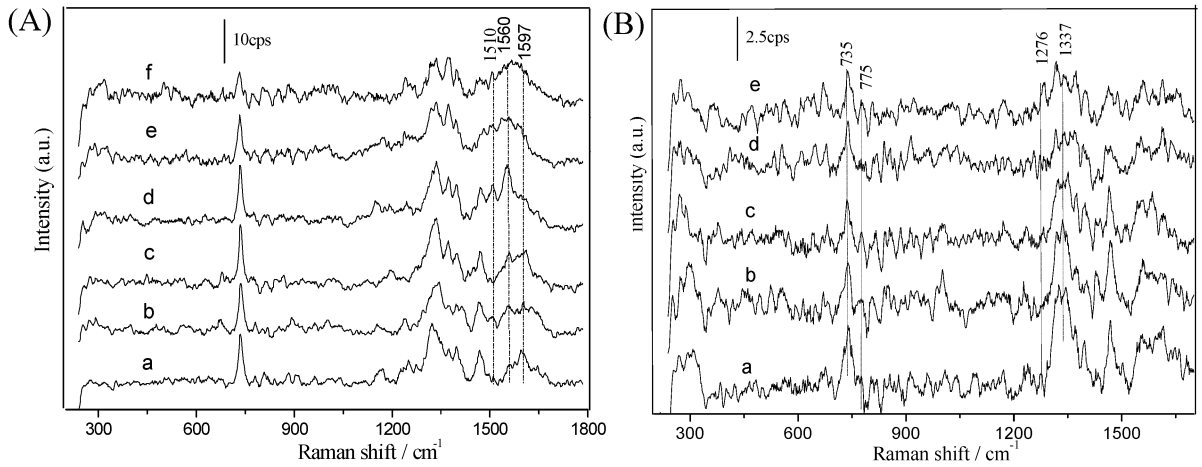

Figure 7. Potential dependence of the SERS spectrum of double-stranded poly(dA)$_{30}$·poly(dT)$_{30}$ adsorbed on the ex-situ roughened gold electrode. (A) 0 (a), −0.2 (b), −0.4 (c), −0.6 (d), −0.8 (e), and −1.0 V (f); (B) 0.1 (a), 0.2 (b), 0.4 (c), 0.6 (d), and 0.8 V (e).

is not via a simple electrostatic interaction between the negatively charged phosphate−deoxyribose backbone and the positively charged electrode surface, whereas that is the case for DNA adsorbed at electrode surfaces via polarization at potentials higher than φ_{pzc} in the DNA solution.[24,27] Therefore, the surface-bound DNA is stable over a wide range of potential, which is also obtained from the above EC−STM investigation.

Second, as shown in Figure 7, although there are no obvious shifts that occurred, the relative intensities of the bands in the SERS spectrum show different enhancement tendencies with the change of the electrode potential. On one hand, this difference is arising from the influence of the electrode potential on the various vibration modes. For example, compared to other bands, the band at 1510 cm^{-1} (−NH bending vibration of T ring[25]) and the band at 1560 cm^{-1} (also attributed to T ring) got enhanced markedly with the negative shift of the electrode potential, whereas the band at 1597 cm^{-1} ascribed to the double-bond stretching vibration of the A ring weakened rapidly with the negative shift of the electrode potential. On the other hand, it suggests that the orientation of the adsorbed bases on the electrode surface undergo a little change with the varying electrode potentials, as can be seen below. Although the SERS enhancement weakened for almost all of the vibration modes, the intensity ratios of the 735 cm^{-1} band to the 775 cm^{-1} band (I_{735}/I_{775}) and the 1337 cm^{-1} band to the 1276 cm^{-1} band (I_{1337}/I_{1276}) tend to diminish when the electrode potential shifted toward the positive direction till close to +0.8 V, which suggests a slight change in the orientation of the base ring plane on the electrode surface.

Conclusion

CV, QCM, and EC−STM techniques are useful tools for profound insight into the nature of DNA attached to surfaces. It has been found that, using the air-drying/adsorption method developed in our laboratory, ds-DNA molecules form a highly ordered and compact monolayer on the gold surface via relatively strong chemisorption where the polymers contact the gold substrate. Nevertheless, ss-DNA molecules cannot form similarly ordered structure. For the first time, information about the way in which ds-DNA molecules are adsorbed on electrode surfaces and the different orientation of bases were obtained at the molecular level by Raman and SERS techniques. The adsorptive orientations of A and T bases are almost invariant over a wide range of potentials, although partial denaturation occurs for the surface-bound ds-DNA because of the different orientations of bases. DNA duplexes will not desorb away from the gold surface even when the potential is far more negative than the potential of zero charge (φ_{pzc}), which distinguishes it from the DNA-immobilized surfaces obtained by the usually adsorptive method. Such a highly ordered and stable ds-DNA monolayer can be used not only for the investigation of interactions between DNA and DNA-targeted molecules but also as an organized nanoscale template for design of functionalized electrode surfaces at mesoscopic level.

Acknowledgment. This work was supported by the National Science Fund for Distinguished Young Scholars (No. 20025311), National Natural Science Foundation of China (Grant Nos. 29773034 and 39770220), Ministry of Education and the State Key Laboratory for Physical Chemistry of Solid Surfaces (Xiamen University, Grant No. 9916). The authors also thank Professor Zhong-Hua Lin, Dr. Bin Ren, Mr. Yong Xie, and Dr. Jian-Zhang Zhou for their kind help.

References and Notes

(1) Chan, V.; Graves, D. J.; Fortina, P.; McKenzie, S. E. *Langmuir* **1997**, *13*, 320.
(2) Livache, T.; Roget, A.; Dejean, E.; Barthet, C.; Bidan, G.; Teoule, R. *Nucleic Acids Res.* **1994**, *22*, 2915.
(3) Nilsson, P.; Persson, B.; Uheén, M.; Nygren, P. A. *Anal. Biochem.* **1995**, *224*, 400.
(4) Herne, T.; Tarlov, M. J. *J. Am. Chem. Soc.* **1997**, *119*, 8916.
(5) Yang, M.; Yau, H. C. M.; Chan, H. L. *Langmuir* **1998**, *14*, 6120.
(6) Levicky, R.; Herne, T. M.; Tarlov, M. J.; Satija, S. K. *J. Am. Chem. Soc*. **1998**, *120*, 9787.
(7) Steel, A. B.; Herne, T. M.; Tarlov, M. J. *Anal. Chem*. **1998**, *70*, 4670.
(8) Mikkelsen, S. R.; Millan, K. M.; Saraullo, A. *Anal. Chem.* **1994**, *66*, 2943.
(9) Huang, E.; Zhou, F. M.; Deng, L. *Langmuir* **2000**, *16*, 3272.
(10) Zhao, Y. D.; Pang, D. W.; Hu, S.; Wang, Z. L.; Cheng, J. K.; Dai, H. P. *Talanta* **1999**, *49*, 751.
(11) Englisch, U.; Gauss, D. H. *Angew. Chem., Int. Ed. Engl*. **1991**, *30*, 613.
(12) Okahata, Y.; Kawase, M.; Niikura, K.; Ohtake, F.; Furusawa, H.; Ebara, Y. *Anal. Chem.* **1998**, *70*, 1288.
(13) Boncheva, M.; Scheibler, L.; Lincoln, P.; Vogel, H.; Akerman, B. *Langmuir* **1999**, *15*, 4317.
(14) Pang, D. W.; Abruña, H. D. *Anal. Chem.* **2000**, *72*, 4700.
(15) Pang, D. W.; Abruña, H. D. *Anal. Chem.* **1998**, *70*, 3162.
(16) Michael, T. C.; Marisol, R.; Bard, A. J. *J. Am. Chem. Soc.* **1989**, *111*, 8901.
(17) Zhao, Y. D.; Pang, D. W.; Hu, S.; Wang, Z. L.; Cheng, J. K.; Qi, Y. P.; Dai, H. P.; Mao, B. W.; Tian, Z. Q.; Luo, J.; Lin, Z. H. *Anal. Chim. Acta*. **1999**, *388*, 93.
(18) Shi, C. H. Master's Thesis, Xiamen University, Xiamen, P. R. China, 1997.

(19) Gao, P.; Gosztola, D.; Leung, L.-W. H.; Weaver, M. J. *J. Electroanal. Chem.* **1987**, *233*, 211.

(20) Hinnen, C.; Rousseau, A.; Parsons, R. *J. Electroanal. Chem.* **1981**, *125*, 193.

(21) Zhang, Z. L.; Pang, D. W.; Zhang, R. Y.; Yan, J. W.; Mao, B. W.; Qi, Y. P. *Bioconjugate Chem.* **2002**, *13*, 104.

(22) Watson, J. D.; Crick, F. H. C. *Nature* **1953**, *171*, 737.

(23) Braun, E.; Eichen, Y.; Sivan, U.; Yoseph-Ben, G. *Nature* **1998**, *391*, 775.

(24) Fang, Y.; Bai, C.; Wang, T.; Zhong, F.; Tang, Y.; Lin, S. B.; Kan, L. S. *J. Mol. Struct.* **1996**, *377*, 1.

(25) Otto, C.; van den Tweel, J. J.; de Mul, F. F. M.; Greve, J. *J. Raman. Spectrosc.* **1986**, *17*, 289.

(26) Kim, S. K.; Joo, T. H.; Suh, S. W.; Kim, M. S. *J. Raman. Spectrosc.* **1986**, *17*, 381.

(27) Fang, Y.; Wei, Y.; Bai, C. L.; Kan, L. S. *J. Phys. Chem.* **1996**, *100*, 17410.

(28) Brabec, V.; Krim, M. H.; Christian, S. D.; Dryhurst, G. *J. Electroanal. Chem.* **1979**, *100*, 111.

(29) Xu, Y. M.; Zhang, Z. Y. *Chinese Sci. Bull.* **1994**, *39*, 1222.

(30) Tsuboi, M.; Ueda, T.; Ushizawa, K.; Sasatake, Y.; Ono, A.; Kainosho, M.; Ishido, Y. *Bull. Chem. Soc. Jpn.* **1994**, *67*, 1483.

(31) Wu, H. Q.; Li, Y. F. *Electrochemistry Dynamics*; Higher Education Press: Beijing, 1998; Vol. 22.